Supporting Information

Three-Dimensional Molecular Mapping of Ionic Liquids at Electrified Interfaces

Shan Zhou[1,2]†, Kaustubh S. Panse[1,2]†, Mohammad Hossein Motevaselian[3]†, Narayana R. Aluru[3]* and Yingjie Zhang[1,2]*

1. Department of Materials Science and Engineering, University of Illinois, Urbana, IL 61801, USA

2. Materials Research Laboratory, University of Illinois, Urbana, IL 61801, USA

3. Department of Mechanical Science and Engineering, University of Illinois, Urbana, IL 61801, USA

†These authors contributed equally to this work

*Correspondence to: yjz@illinois.edu (Y.Z.) or aluru@illinois.edu (N.R.A.)

1. Cyclic voltammetry and charge density quantification

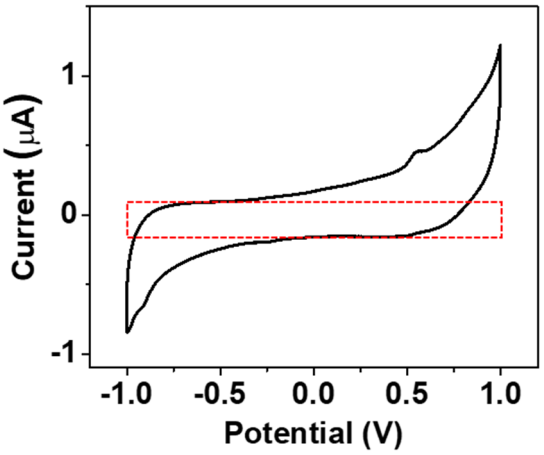

Figure S1. CV of EMIM-TFSI on HOPG in the potential range of -1 V – 1 V (*vs* Pt). Scan rate: 10 mV/s. Red dashed rectangle represents the area used to calculate the amount of capacitive charges, where the parasitic redox current was not included. The extracted capacitive charge density over the full CV cycle is ~4.8 charges per nm^2. Using this method, we consistently obtain similar capacitive charge density at different scan rates.

2. AFM images of HOPG surface

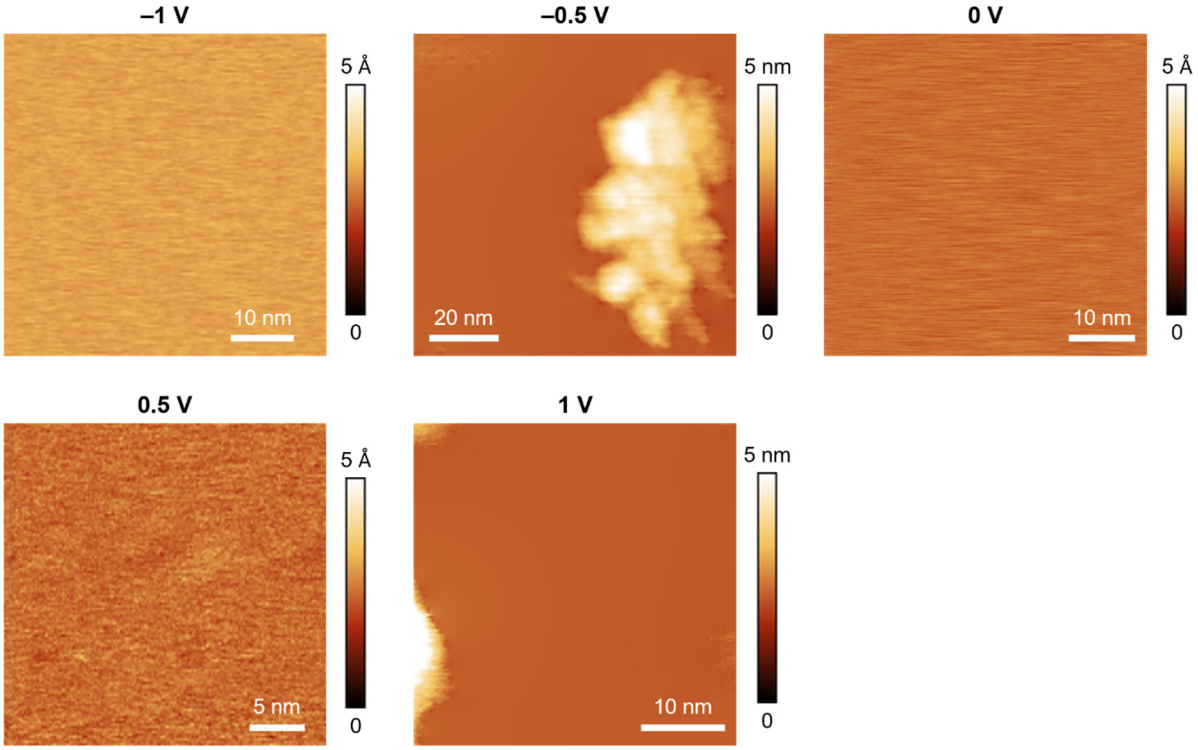

Figure S2. Large area AFM height images of the HOPG surface immersed in EMIM-TFSI, acquired at different potentials (*vs* Pt). Note that different images are obtained at different areas, and do not represent continuous evolution of surface topography features at different potentials. Most areas are clean and flat, and molecular cluster features are only occasionally observed at any potential within -1 V – 1 V (*vs* Pt).

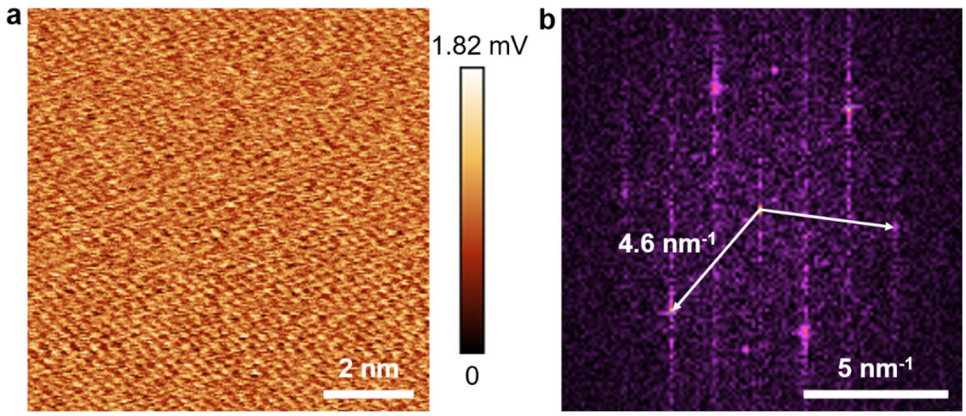

Figure S3. Small area lattice-resolution images. (a) AFM lateral signal of the HOPG surface immersed in EMIM-TFSI, at 0 V *vs* Pt. (b) The corresponding Fourier transform image.

3. DC mode EC-3D-AFM data analysis procedures

The observables obtained from EC-3D-AFM measurements are cantilever deflection (*Defl*) *vs* scanner extension (*Ext*) at each (x, y) position. Typical separation between nearest x and y points is ~1.56 Å. At each (x, y) point, 50000 *Ext* points (including approach and retraction) are acquired over a range of 5–10 nm.

We first calibrate the InvOLS (inverse optical lever sensitivity) at each (x, y) position by extracting the slope of the retraction part at the end of each *Defl vs Ext* curve and normalizing this slope value to 1. All the InvOLS values in each x-z frame are then averaged and used to correct the *Defl* values at individual (x, y) position in the frame (Figure S4a). We further obtain the z values using $z = Defl - Ext$ and the corresponding force values as $F = k \cdot Defl$ (where k is the spring constant of the cantilever), at each (x, y) position. We then apply a z offset so that the average z value of the ending part of the approach curve is 0, and a force offset so that the beginning part of the approach curve has an average force of 0. An example of one calibrated force-z curve is shown in Figure S4b. Only the approach curves are used to further process the histograms and count maps.

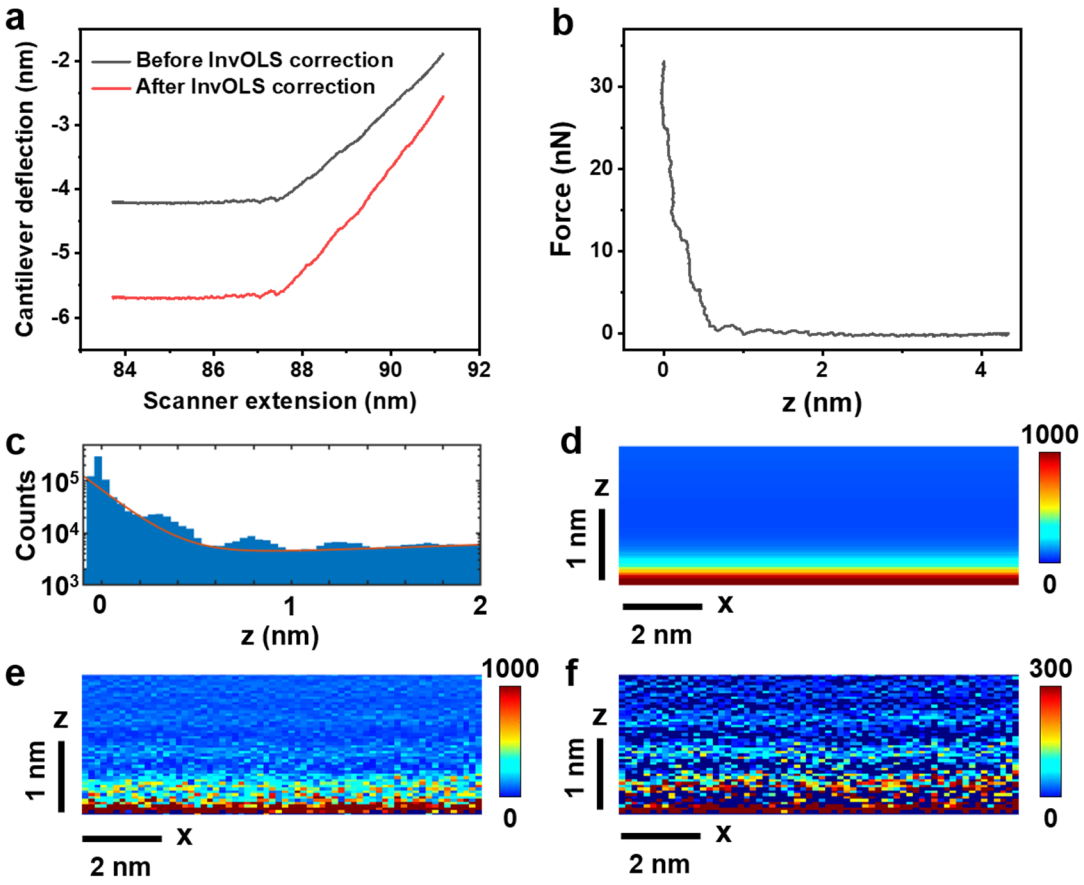

Figure S4. Detailed procedures of the EC-3D-AFM data analysis. All the results are obtained at 0 V *vs* Pt, as examples to illustrate the data processing steps. (a) A *Defl vs Ext* curve at one (x, y) spot before and after correcting the InvOLS value. (b) The corresponding force-z curve. (c) 1D histogram of one x-z frame and its corresponding double-exponential fit to the local minima

(orange curve). (d) 2D background generated using the exponential fit from (c). (e) and (f) are x-z count maps before and after subtracting the 2D background (as shown in (d)), respectively.

After obtaining Force *vs* z curves at each (x, y) point, we use all the z values in a full x-z frame to obtain the 1D count histogram, as shown in Figure S4c. The histogram is generated across the z range of –0.1 to 3.9 nm with 100 bins (we only show the results up to 2 nm in the figures). In order to highlight the features with higher counts, we perform a double-exponential fit to the local minima of the 1D histogram, using the equation: $Counts=ae^{bz}+ce^{dz}$, with a, b, c, and d as fitting parameters (Figure S4c). This fitted function is normalized by the number of x points in each x-z frame to generate a smooth 2D background for the x-z count map (Figure S4d).

A raw x-z count map (with no background subtraction) is shown in Figure S4e. This map has 64 × 100 pixels over a 10 × 4 nm^2 range in the x-z cross section frame (we only show the lower half of the map to highlight the EDLs near the interface). The point count density near the HOPG surface (*i.e.*, z<0.5 nm) tend to increase dramatically as the z becomes lower, which is mainly due to the sinusoidal z motion during the 3D-AFM measurements, in addition to the higher molecular density near the interface. To remove the background effects and improve the color contrast of EDLs, we subtract the smooth 2D background (the one shown in Figure S4d) from the raw x-z count map, to obtain a new point count map, as shown in Figure S4f. All the reported x-z count maps of DC mode 3D-AFM in this paper, unless otherwise mentioned, are generated using the same overall procedure as that of Figure S4f. The y-z maps shown in Figure 2a are obtained using the same method, except that the deflection calibration and background subtraction are performed based on individual y-z frames, instead of x-z frames.

For the 3D count maps at five different voltages in the movies provided in the online supporting information, we perform the deflection calibration and background subtraction based on the x-z frames of the 3D data matrix, and then plot the x-z, y-z and x-y count maps in 3D view.

4. AC mode EC-3D-AFM procedures and results

4.1 Measurement procedures

AC mode AFM measurements are performed using a Cypher ES AFM, the same system used in DC mode AFM. AFM probes (PPP-NCHAuD, manufacturer: Nanosensors) are purchased from NanoAndMore USA Inc. The tip is composed of Si/SiO_2 which is electrically insulating. Before each EC-3D-AFM experiment, we obtain the spring constant by performing thermal tune of the probe in air. The NCH tips have typical spring constants of 34 – 45 N/m. The tip used to generate the results reported in Figure S6 has k = 37.41 N/m. Once the probe is immersed in liquid, we perform thermal tune again to obtain the InvOLS value. This value is 23.4 nm/V. The cantilever is driven at resonance for AC mode imaging, including both 2D imaging of the HOPG surface and 3D-AFM mapping of the EDLs. The 3D motion, voltage control and tip monitoring protocols are the same as those used in DC mode EC-3D-AFM measurements. Using AC mode 3D-AFM, we record cantilever amplitude and phase as a function of the 3D probe position. To

ensure that the probe can reach the HOPG surface, the amplitude setpoint is chosen to be ~20% of the free amplitude and the phase reaches ~60° at the lowest point.

Based on the cantilever tune results in air and in liquid, we observe strong oscillation damping in the ionic liquid environment (Figure S5).

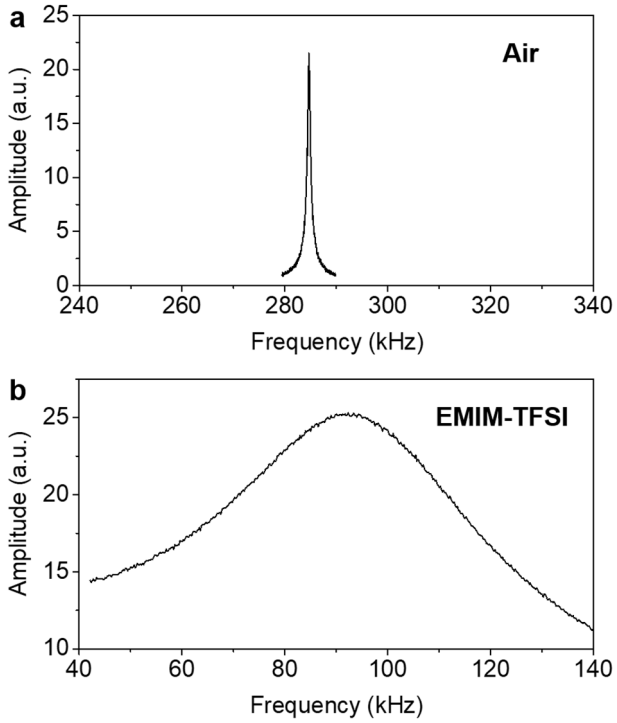

Figure S5. Cantilever tune of a PPP-NCHAuD probe in air (a) and in EMIM-TFSI (b), revealing a large reduction of resonance frequency (from 284.7 kHz to 92.1 kHz) and quality factor (from 599.2 to 1.7) when the environment is changed from air to the IL.

4.2 Analysis procedures

The observables obtained from AC mode measurements are amplitude (*Amp*) and phase (*Phase*) *vs* scanner extension (*Ext*) at each (x, y) position. 50000 *Ext* points, including approach and retraction, are acquired over a typical range of 3–3.5 nm at each (x, y). Only the approach curves are used to further process the AC mode x-z maps.

We first correct the amplitude values using InvOLS obtained from the thermal tune result in liquid. For each x-z frame, we obtain the *Amp* and *Phase* values averaged over all the x positions at each *Ext*. We further obtain the z values at each (x, y) point using $z = -Ext - Amp$. After that, a z offset is applied so that the z value of the ending part of the approach curve is 0, and *Phase* values are then plotted *vs* the new z. A linear interpolation is performed so that the z values have uniform spacing in the range of 0–2.5 nm.

In order to highlight the EDL features, we perform a double-exponential fit to the average *Phase vs* z in each x-z frame, using the equation: $Phase = ae^{bz}+ce^{dz}$, where a, b, c, and d are fitting parameters. This phase background curve is then subtracted from the individual *Phase vs* z curve at each (x, y) location. The *Phase vs* z curves after background subtraction are further averaged over every 50 z points, and then used to plot the x-z maps as shown in Figure S6a.

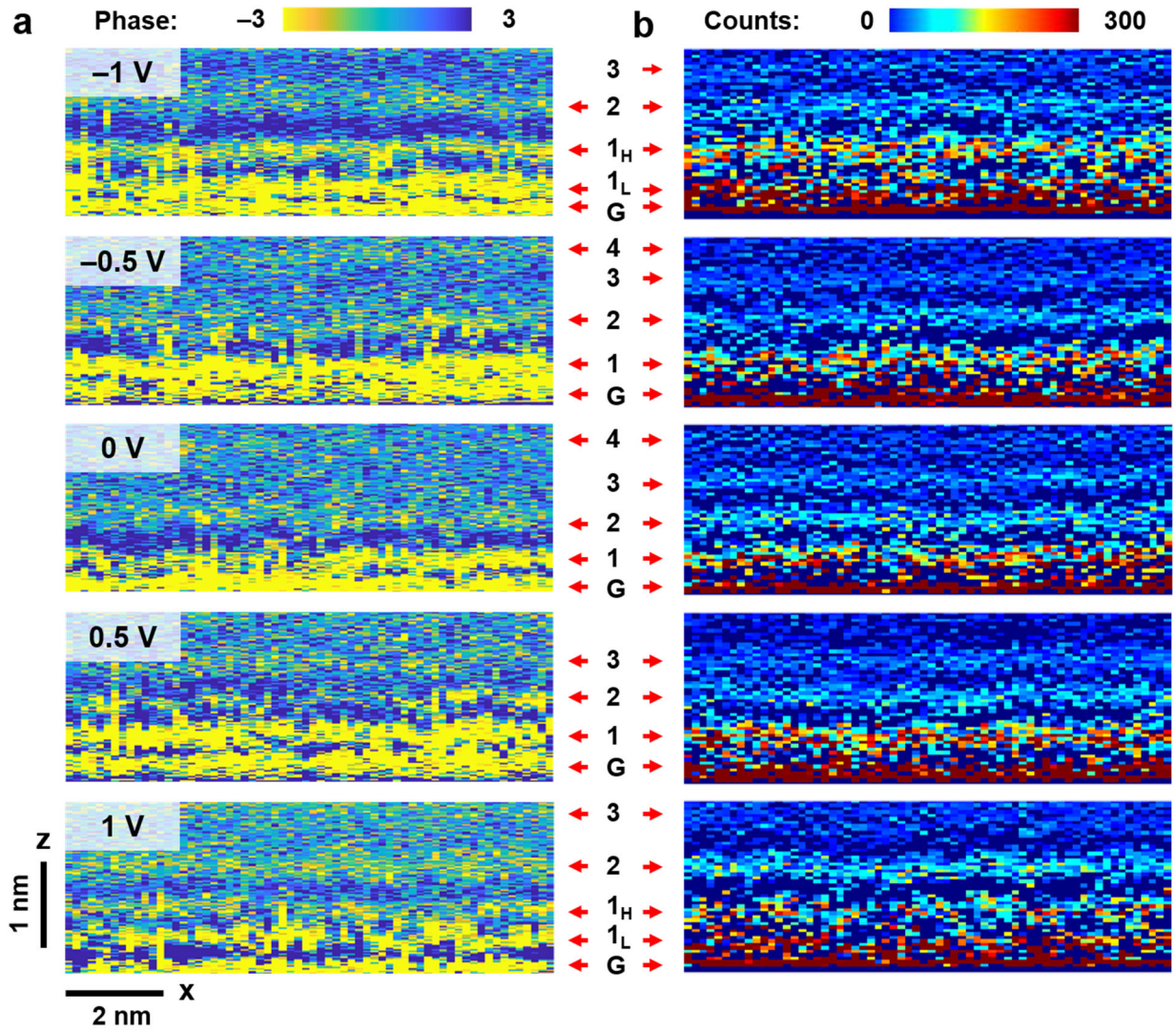

Figure S6. Comparison of AC mode (a) and DC mode (b) xz maps of EMIM-TFSI on HOPG using the same EC-3D-AFM system, at a series of different electrode potentials (*vs* Pt). In the AC mode maps, lower phase (yellow color) roughly corresponds to higher force and thus higher molecular density.[1,2]

5. Configuration of the molecular dynamics simulation

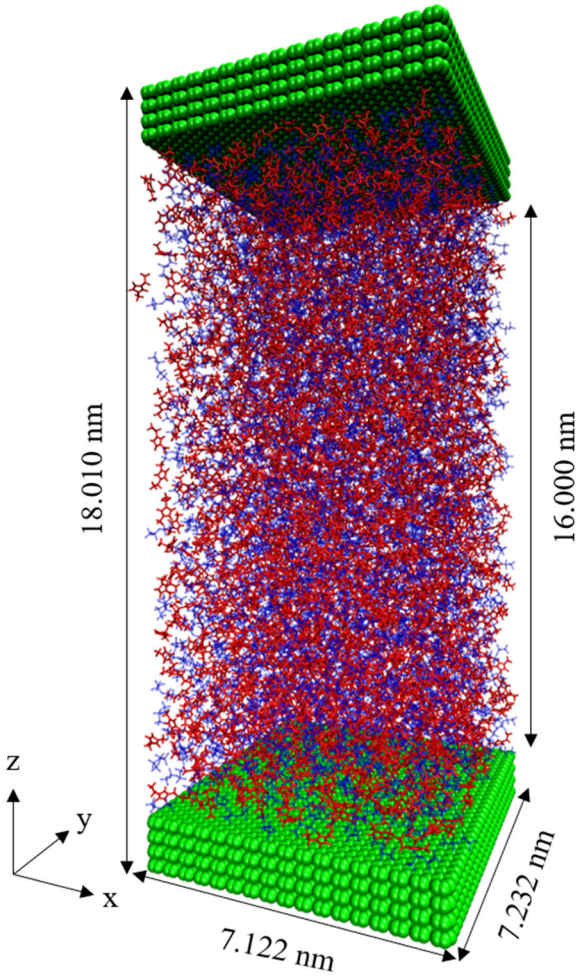

Figure S7. Snapshot of the graphite/EMIM-TFSI/graphite system in MD simulation. The graphite carbon atoms are shown in green color. The $EMIM^+$ and $TFSI^-$ ions are represented by red and blue colors, respectively.

6. Simulated charge and potential profiles

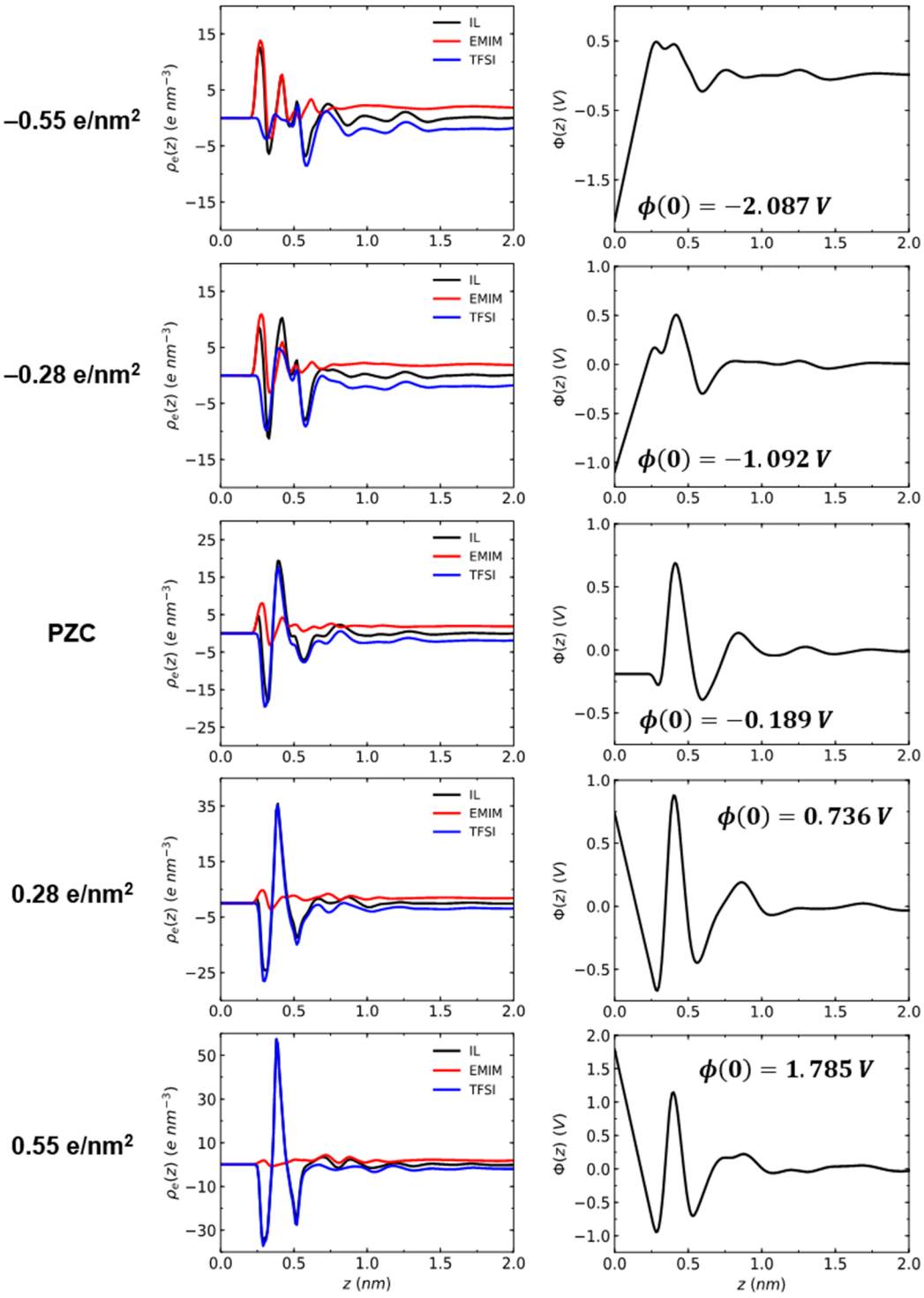

Figure S8. MD simulation results of the charge density and potential distribution in the EMIM-TFSI electrolyte as a function of the distance from the electrode surface. The obtained potential values at the electrode surface are shown on the figures. From the differences of the potential values, we find that the systems with surface charge densities of ±0.28 e/nm^2 and ±0.55 e/nm^2

have electrode potentials of PZC + 0.93 V, PZC – 0.90 V, PZC + 1.97 V, and PZC – 1.90 V, respectively.

7. Photos of the liquid cup of the electrochemical cell

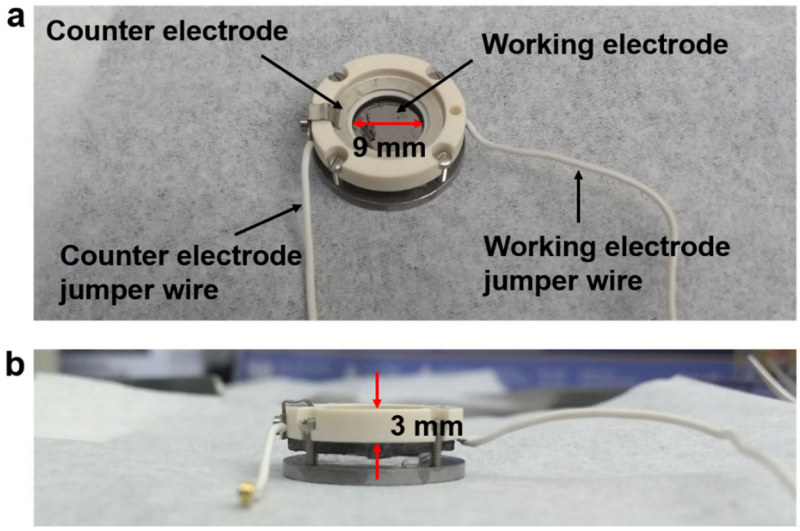

Figure S9. Photos of the liquid cup, a key part of the sealed AFM electrochemical cell. (a) top view. (b) side view.

8. Optical image of the probe

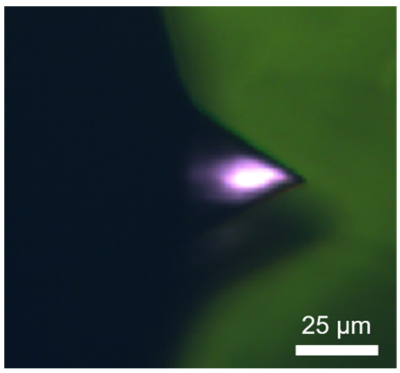

Figure S10. Optical image of the FS-1500AuD probe immersed in EMIM-TFSI in the AFM EC cell, with the laser focused on the cantilever.

References

(1) Uhlig, M. R.; Martin-Jimenez, D.; Garcia, R. Atomic-Scale Mapping of Hydrophobic Layers on Graphene and Few-Layer MoS_2 and WSe_2 in Water. *Nat. Commun.* **2019**, *10*, 2606.

(2) Martin-Jimenez, D.; Chacon, E.; Tarazona, P.; Garcia, R. Atomically Resolved Three-Dimensional Structures of Electrolyte Aqueous Solutions near a Solid Surface. *Nat. Commun.* **2016**, *7*, 12164.